New Technique to Measure Transmission Line Attenuation

J. Carroll, M. Li, and K. Chang

***Abstract*—A new technique using a quarter-wave open stub resonator was developed to measure a transmission line's attenuation coefficient. Transmission line attenuation was extracted from the Q-factor measurement of the open stub resonator. Equations were derived that relate the stub's two port S-parameters to transmission line attenuation. The new method's benefits include higher accuracy over other methods of attenuation measurement, less area required for the test structure, and easier test structure design. Applications include simple and accurate determination of the transmission line's loss characteristics and effective dielectric constant at very high frequencies.**

I. Introduction

High frequency designers need accurate characterization of circuit components in order to meet circuit specifications in as few design iterations as possible. One of the most difficult characteristics to theoretically determine is transmission line attenuation. However, it can be easily measured. A common method is to find the Q-factor of half-wave transmission line resonators [1]. Typically, the $S21$ measurement of a half wave resonator around resonance, shown in Fig. 1(a) for microstrip, is used to determine the transmission line's attenuation. This paper describes a new test structure using a quarter-wave open stub resonator, shown in Fig. 1(b) for microstrip, that is a more accurate and useful topology for characterizing planar transmission lines.

The Half Wave Line Resonator Method (HWLRM) has many inherent problems. First, the size of the resonator and required feed lines take up a large amount of substrate area. For example, GaAs "real-estate" is expensive and may prohibit the use of HWLRM to monitor transmission line attenuation on production wafers. Likewise, the long length of the structure can cause measurement problems with wafer probe stations. Secondly, the HWLRM coupling gaps shown in Fig. 1(a) cause measurement inaccuracies at high frequencies due to radiation losses. The two gaps are actually four open radiating microstrip ends, whose large radiation losses at high frequencies are undesirably included in the measured transmission line attenuation coefficient. Therefore, a new test structure was developed in order to save space, reduce radiation, and improve transmission line characterization. This paper describes the derivation of the new method's extraction of attenuation and effective dielectric constant. Both test structures shown in Fig. 1 were constructed with microstrip to verify the new technique and determine any measurement differences.

II. Derivation of Open Stub Q-Factor

The new test structure involves the use of a quarter-wave stub resonator shown in Fig. 1(b). The new topology reduces the amount of space needed for the test structure by at least 50% over the HWLRM. The quarter-wave resonator can be realized through the use of an open circuited quarter-wave transmission line stub. The new test structure is directly coupled to the measurement system which avoids the inaccuracies caused by the HWLRM's coupling gaps. There is only one open end in the new structure, which eliminates most of the radiation and discontinuity losses found in the HWLRM. The quarter-wave stub resonator method does introduce a tee-junction discontinuity which adds a small amount of capacitance to the stub [2] thereby lowering the stub's resonant frequency. Simulations have shown that this frequency shifting is less than 1% for 50-Ohm stubs at 3 GHz on a substrate dielectric constant of 2.3. This is much less than the 5% frequency shift predicted on the same substrate by the HWLRM's inherent lengthening due to the straight resonator's open ends [3].

The open circuit transmission line stub creates an $S21$ band-stop response. This can be modeled by replacing the stub with the lumped element resonator circuit as shown in Fig. 2 at or near the stub's resonance. The following equation gives the $S21$ of the 2 port network in Fig. 2 at or near resonance [4]:

$$S21 = \frac{2Z_{\text{in}}}{2Z_{\text{in}} + Z_0} \tag{1}$$

where Z_0 is the characteristic impedance of the measurement system and Z_{in} is the equivalent input impedance of the lumped element resonator shown in Fig. 2. It would be convenient to measure some $S21$ points off resonance ($S21_{\text{RES}}$) which correspond to the "twice power" points. The "twice power" points are those when the magnitude of $S21$ is equal to the $S21_{\text{RES}}$ times square root of 2

$$|S21_{\text{twice-power}}| = \sqrt{2}\,|S21_{\text{RES}}|. \tag{2}$$

Equation (2) can be written using $S21$ from (1) and an insertion loss measurement at resonance ($S21_{\text{RES}}$). $S21_{\text{RES}}$ is entirely real because resonance is defined as when the imaginary components of the resonator cancel and the imaginary part of $S21$ is equal to zero. Substituting (1) into (2) gives

$$\left|\frac{2Z_{\text{in}}}{2Z_{\text{in}} + Z_0}\right| = \sqrt{2}\,S21_{\text{RES}}. \tag{3}$$

The input impedance Z_{in} given by $R_0(1 + j2Q_0\Delta\omega/\omega_0)$ for a series lumped circuit [5] can be substituted into (3) . This leads to

$$\frac{\left|2R_0\left[1 + j\left(\frac{2Q_0}{\omega_0}\Delta\omega\right)\right] + Z_0\right|}{\left|R_0\left[1 + j\left(\frac{2Q_0}{\omega_0}\Delta\omega\right)\right]\right|} = \frac{\sqrt{2}}{S21_{\text{RES}}} \tag{4}$$

where Q_0 is the unload Q-factor of the resonator, ω_0 is the resonant frequency, $2\,\Delta\omega$ is the "twice power" bandwidth. R_0 in (4) can be found at resonance by a magnitude measurement of $S21_{\text{RES}}$ similar to the DeLoach measurements for equivalent parameters of diodes [6]. The loaded $Q(Q_L)$ is defined as the resonant frequency divided by the resonator's 3 dB bandwidth and is given below

$$Q_L \equiv \frac{\omega_0}{2\Delta\omega}. \tag{5}$$

Using (5), taking the magnitudes of the numerator and denominator of the left hand side of the simplified (4). and with substitution of (1) will yield:

$$Q_0 = \frac{Q_L}{\sqrt{1 - 2|S21_{\text{RES}}|^2}}. \tag{6a}$$

Another form of the equation can be expressed as

$$Q_0 = \frac{Q_L}{\sqrt{1 - 2 \cdot 10^{-(L_A/10)}}} \tag{6b}$$

where L_A is the insertion loss in dB at the resonance. Equation (6a) or (6b) can be used to extract the unloaded Q of a quarter-wave stub resonator with a simple magnitude measurement of insertion loss at the resonant frequency and its "3 dB up" bandwidth. Equation (6)

Manuscript received September 23, 1993; revised March 3, 1994.

The authors are with the Department of Electrical Engineering, Texas A&M University, College Station, Texas 77843-3128 USA

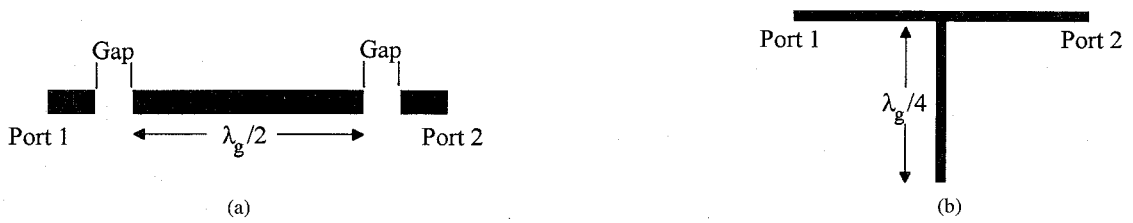

Fig. 1. Top View of the Microstrip Test Structures used for Attenuation Measurement. (a) Half-Wave Line Resonator Method (HWLRM) structure. (b) Quarter-Wave Stub Resonator structure.

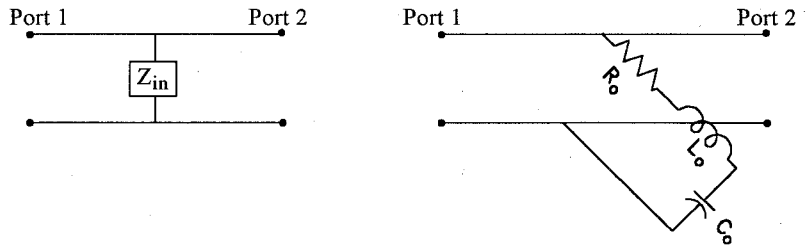

Fig. 2. Quarter-wave stub equivalent circuit.

shows that the unloaded Q for a normal transmission line quarter-wave stub is nearly equal to the loaded Q. For example, if the magnitude of $S21_{\mathrm{RES}}$ is 0.3 (-30 db), the square root term in (6) equals to 0.9991. Little error occurs by using one for the square root term. The error in this approximation becomes even less for low transmission line losses. This characteristic of the quarter-wave method of determining Q occurs because the measurement system has little effect on the Q of the open stub. This is not the case for the HWLRM whose unloaded Q-factor is given by [7]

$$Q_0 = \frac{Q_L}{1 - 10^{-(L_A/20)}} \tag{7}$$

where L_A is the insertion loss of the half-wave resonator in dB at resonance. This equation was derived for lightly-coupled parallel resonator structures which models the bandpass nature inherent in the HWLRM.

The transmission line's effective dielectric constant can then be determined through the resonant frequency and the known length of the quarter-wave stub. The effective dielectric constant at the frequency of each of the stub's quarter-wave resonances is given below, similar to the HWLRM structure's expression [8].

$$\mathcal{E}_{\mathrm{meas,eff}} = \left(\frac{\mathrm{nc}}{4f_{\mathrm{RES}}(l + l_e)}\right)^2 \quad n = 1,\ 3,\ 5, \ldots \tag{8}$$

where c is the free space speed of light. This equation takes into effect the fringing at the end which effectively lengthens the physical length of the resonator (l) by an extra length (l_e) which can be determined by well known empirical equations [3]. Finally, the measured Q-factor is used in the following equation along with the effective dielectric constant to calculate the transmission line attenuation as in the HWLRM [1]

$$\alpha_0 = \frac{8.686\pi f_{\mathrm{RES}}\sqrt{\mathcal{E}_{\mathrm{eff}}}}{cQ_0}. \tag{9}$$

The units for α_0 are in dB/length. The calculation for the error bounds on both the quarter-wave Q-factors and attenuation coefficients are the same as derived by Goldfarb and Platzker [1].

III. Simulation and Measurement of Resonator Structures

The derived equations were tested by Touchstone CAD simulation of both the HWLRM and our method. The structures shown in Fig. 1 were simulated on Duriod substrate ($\mathcal{E}_r = 2.3$, height = 62 mil, normalized bulk resistivity RHO = 6). The simulations of the microstrip included only the microstrip conduction losses and did not include discontinuity or radiation losses caused by the resonator structures themselves. The loaded and unloaded Q determined for the quarter-wave open stub are both 292. With the same microstrip parameters, the HWLRM gave a loaded Q of 291.5 and an unloaded Q of 292.7. These simulated measurements were close enough to be considered equal considering numerical and interpolation accuracy. The simulated measurement demonstrated that the quarter-wave stub technique can successfully determine the same unloaded Q of a microstrip transmission line as does the HWLRM.

The simulated structures were constructed on the Duriod substrate to compare the measured Q-factors and attenuation coefficients. The measured values will differ from the simulated data in that radiation and discontinuity losses are undesirably included in the unloaded Q factors. This inclusion reduces the measured Q-factor and increases the measured attenuation from the true transmission line characteristics. A broad sweep over frequency on the structures shown in Fig. 1 was used to find their resonance. A very narrow sweep was then used to ensure low measurement error. All Q-factors were measured at no more than 0.5 MHz steps to keep the measurement error less than $\pm 3\%$ for the Q-factors lower than 100, and less than $\pm 6\%$ for the other higher Q-factors [1]. The measured results are listed in Table I and show that the unloaded Q-factor in the HWLRM is not repeatable for different size gaps. This led to the microstrip with 100-mil gaps to have a 13% different unloaded Q-factor than the tighter coupled 50-mil gap resonator. The difference is greater than the $\pm 3\%$ error bounds on both of the measurements. The sensitivity of the HWLRM structures to errors in measurement causes this measurement inaccuracy. The quarter-wave stub resonator method does not exhibit this measurement error because it has no coupling gaps and less radiation loss. Table I also shows the 50-mil gap HWLRM had 49% less Q-factor than the open stub resonator. The HWLRM measurement must include more losses than the quarter-wave stub resonator measurement because the CAD simulations did not predict this large difference between these two Q factor measurement techniques. Table I shows that the lower Q of the HWLRM causes the extracted attenuation measurement to be higher than the quarter-wave stub resonator measurement although the effective dielectric constants are nearly the same. Therefore, it

TABLE I
MEASURED RESONATOR RESULTS USING LOW DIELECTRIC CONSTANT SUBSTRATE ($\mathcal{E}_r = 2.3$)

Resonator/Structure Type	Resonant Frequency (GHz)	S21 (dB)	Loaded Q	Unloaded Q	Attenuation dB/m	Effective Dielectric Constant
HWLRM 50 mil gap	3 486	-12 31	75 4	99.5	3 791	1 473
HWLRM 100 mil gap	3 506	-25 02	81 9	86 8	4 299	1 465
Quarter-Wave Stub	3 390	-44 84	196 7	196 7	1 881	1 44

TABLE II
MEASURED RESONATOR RESULTS USING HIGH DIELECTRIC CONSTANT SUBSTRATE ($\mathcal{E}_r = 10.5$)

Resonator/Structure Type	Resonant Frequency (GHz)	S21 (dB)	Loaded Q	Unloaded Q	Attenuation dB/m	Effective Dielectric Constant
HWLRM	2 878	-12 81	145 4	188 5	2 486	2.768
Quarter-Wave Stub	3 097	-40 88	184 2	184 2	2 493	2 657

was thought that the differences were caused by larger discontinuity and radiation losses inherent in the HWLRM structure.

Two experiments were run to verify if radiation was the cause of the Q-factor differences. The first experiment was to build the test structures on a Duriod substrate with a dielectric constant of 10.5 in order to suppress the radiation of the gaps. The resonator structure's dimensions were redesigned so that the resonances stayed at about 3.5 GHz. The test results in Table II show a much closer agreement between the HWLRM and quarter-wave stub resonator methods. The difference between them is within the measurement uncertainty.

The resonator structures were then tested in an anechoic chamber to determine how much power they radiated by measuring their directive gain. Both types of resonators were terminated at one port with 50 Ω and each of the radiation patterns was taken from the other port at the resonant frequencies listed on Table I. The E-Plane patterns in Fig. 3 for the low dielectric constant of 2.3 show that the open stub resonator structure radiates 11.2 dB less power at its first resonance than the half wave line resonator does with the 50-mil gap. The 100-mil gap half wave line resonator exhibited an even larger amount of radiation. The radiation differences show that the HWLRM resonant structure radiates much more total power than the quarter-wave stub structure for low dielectric constants which caused the difference in the two method's Q-factors. The HWLRM structure actually exhibits a small amount of directive gain (0.12 dB), which shows it radiates too much for accurate transmission line attenuation measurement. The radiation patterns for the higher dielectric constant of 10.5 were also measured and exhibited a reduction in radiation by both test structures. The quarter-wave stub structure showed a 3-dB decrease in radiation to -18.4 dB at boresight. The HWLRM structure showed a substantial radiation decrease to -14 dB. However, there was still a 4.4 dB higher radiation for the half-wave resonator than the quarter-wave stub. This led to the much closer measured Q-factors exhibited in Table II. The quarter-wave stub resonator still radiated less, but the power levels were so low that the difference was not seen in the Q-factor measurement.

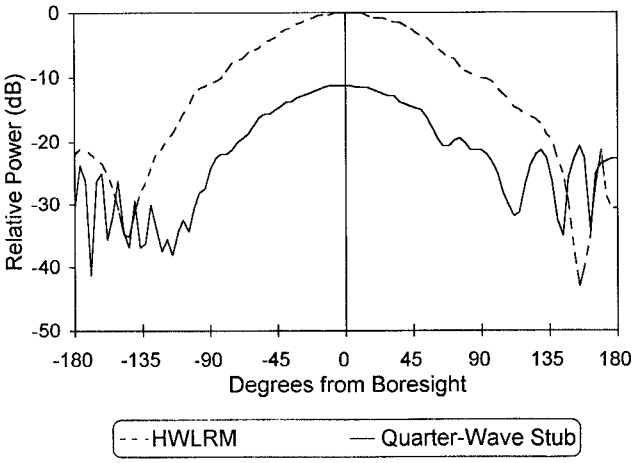

Fig. 3. E-plane radiation patterns from both resonators (HWLRM structure and quarter-wave stub resonator structure).

IV. MEASUREMENT TECHNIQUE DIFFERENCES

In Section III, it was shown that the HWLRM was very sensitive to the measurement system and coupling gaps. Table I shows that the HWLRM's measurement sensitivity causes the unloaded Q-factor to be inaccurate for different gap sizes. Also, only empirical equations and rules of thumb are available to determine which gaps cause too much or too little coupling to prevent measurement system's influence in the Q-factor measurement [8]. This uncertainty causes the designing of the half wave resonators to be done with a best guess. Designing the quarter-wave structure is easier due to its direct coupling to the measurement system. The gaps in the HWLRM method were also shown to radiate much more than the quarter-wave resonator, which resulted in different measured Q-values. When this HWLRM radiation was suppressed with a high dielectric constant substrate, the two method's Q-values converged. The radiation causes the HWLRM to be less accurate than the open stub method especially for low dielectric constant substrates and low loss transmission lines. Finally, the quarter-wave stub resonator structure takes up at least 50% less area than the HWLRM and therefore is easier to measure and less costly to produce on expensive substrates such as GaAs.

V. CONCLUSION

A new test structure using a quarter-wave open stub resonator for attenuation measurement of transmission lines was developed. The equations describing the extraction of the unloaded Q-factor, attenuation, and effective dielectric constant were derived for the quarter-wave open stub resonator measurement method. Theoretical verification was done in comparison with the common half-wave measurement on microwave circuit simulation software. Microstrip examples of both structures were built on low and high dielectric constant substrates to demonstrate that the quarter-wave measurement is more accurate. Other advantages of using the quarter-wave resonator method are that it is easier to design and takes up less space than the half wave resonator method. This new structure demonstrated in this paper will allow the measurements of the Q-factor, attenuation, and effective dielectric constant of any type of transmission line, such as microstrip, coplanar waveguide or stripline.

ACKNOWLEDGMENT

The authors would like to thank Hewlett-Packard and the Rogers Corporation for their donations of measurement equipment and materials used in this research. The authors would also like to acknowledge Alex and Diana Kirk for reviewing this paper.

REFERENCES

[1] M. Goldfarb and A. Platzker, "Losses in GaAs microstrip," *IEEE Trans. Microwave Theory Tech.*, vol. 38, no. 12, pp. 1957–1963, Dec. 1990.
[2] T. C. Edwards, *Foundations for Microstrip Circuit Design.* New York: John Wiley & Sons, 2nd ed, 1992, pp. 145–149.
[3] M. Kirschning, R. H. Jansen and N. H. L. Koster, "Accurate model for open end effect of microstrip lines," *Electron. Lett.*, vol. 17, no. 3, pp. 123–125, Feb. 1981.
[4] G. Gonzalez, *Microwave Transistor Amplifiers.* Englewood Cliffs: N.J., Prentice-Hall, 1984, pp. 18–19.
[5] D. Pozar, *Microwave Engineering.* Reading MA: Addison-Wesley, p. 332, 1990.
[6] B. DeLoach, "A new microwave measurement technique to characterize diodes and an 800-Gc cutoff frequency varactor at zero volts bias," *IEEE Trans. Microwave Theory Tech.*, vol. MTT-12, no. 1, pp. 15–20, Jan. 1964.
[7] K. Chang, F. J. Hsu, J. Berenz and K. Nakano, "Find optimum substrate thickness for millimeterwave GaAs MMICs," *Microwaves & RF*, vol. 23, no. 9, pp. 123–128, Sept. 1984.
[8] T. C. Edwards, *Foundations for Microstrip Circuit Design.* New York: John Wiley & Sons, 2nd ed., 1992, pp. 254–255.

Waveguide and Resonator Perturbation Techniques Measuring Chirality and Nonreciprocity Parameters Biisotropic Materials

Sergei A. Tretyakov and Ari J. Viitanen

***Abstract*—Waveguide and resonator perturbation techniques are considered for determining electromagnetic parameters of general biisotropic, or nonreciprocal chiral, materials. The biisotropic materials are the most general linear isotropic media, whose constitutive relations are governed by four complex material parameters. The material parameters of biisotropic media can be obtained through measuring the change in the propagation constant of waveguide modes or measuring the shift in the resonant frequency for resonators with perturbation techniques. To measure these parameters a method utilizing waveguides or cavity resonators with two degenerate modes is proposed.**

I. INTRODUCTION

Interest in biisotropic materials has been recently widely increasing since they offer some novel promising applications in microwave technology and radio engineering, like low-reflection coatings [1], elimination of crosspolarization in microwave lens antennas [2] and construction of a twist polarizer [3]. The most general isotropic materials are characterized by four material parameters, dielectric permittivity, magnetic permeability, chirality parameter and nonreciprocity parameter. The biisotropic media are, in general, nonreciprocal, and the reciprocal special case is usually called chiral media. In electromagnetics terms, biisotropic materials were formalized for the first time in 1948, when Tellegen invented gyrator, a nonreciprocal circuit element, and considered what kind of material is needed to manufacture it [4]. It has been known that the material parameters of a biisotropic medium are associated with a model of the medium possessing both electric and magnetic dipole moments, parallel or antiparallel to each other [5].

To be able to determine the medium parameters of the biisotropic material is of great importance for practical applications. This work applies to chiral media in practice and gives a method to determine the material parameters for the general, theoretically interesting biisotropic media. In this paper we use the perturbation theory for general waveguides and resonators with small biisotropic inclusions and propose possible cavity resonator measurement techniques and waveguide perturbation techniques for measuring both the chirality parameter and the nonreciprocity parameter simultaneously. Free-space techniques are used to measure the chirality parameter in chiral composites [6]–[8], and the theoretical basis for the retrieval of the material parameters is the theory of reflection and transmission in chiral slabs. An alternative measurement technique for nonreciprocity parameter measurements is given in [9]. An approach to determination of the chirality parameter by using corrugated waveguides with chiral inclusions is discussed in [10]. A cavity resonator method for measuring the nonreciprocity parameter has been suggested in [11].

Manuscript received March 8, 1993; revised April 11, 1994.

S. Tretyakov is with the Radiophysics Department, St. Petersburg State Technical University, 195251, Polytekhnicheskaya 29, St. Petersburg, Russia

A. Viitanen is with the Electromagnetics Laboratory, Department of Electrical Engineering, Helsinki University of Technology, Otakaari 5 A, FIN-02150 Espoo, Finland.

IEEE Log Number 9406785.

II. PERTURBATION THEORY

The biisotropic medium is characterized by linear and isotropic constitutive relations with four scalar parameters. These relations can be written (assuming the $e^{j\omega t}$ time dependence), in the form

$$\bar{D} = \epsilon\bar{E} + \xi\bar{H}, \qquad \bar{B} = \mu\bar{H} + \zeta\bar{E}, \tag{1}$$

where ϵ and μ are dielectric permittivity and magnetic permeability of the medium, respectively, and the parameters ξ and ζ characterize coupling between the electric and magnetic fields. It is convenient to write the coupling parameters ξ and ζ in the form [12]:

$$\xi = (\chi - j\kappa)\sqrt{\mu_o\epsilon_o}, \qquad \zeta = (\chi + j\kappa)\sqrt{\mu_o\epsilon_o}, \tag{2}$$

where ϵ_o and μ_o are the free-space permittivity and permeability, respectively, and the parameter κ describes the magnitude of chirality and χ the nonreciprocity of the medium.

A. Waveguide Perturbation

Consider a waveguide with an arbitrary cross-section and ideally conducting walls. Field vectors of propagating modes in the empty guide have $e^{-j\beta_o z}$ dependence on the longitudinal co-ordinate z. A biisotropic rod of a small cross-section positioned in the waveguide causes a small change $\Delta\beta$ in the propagation factor β_o which can be measured. The unperturbed electric and magnetic fields $\bar{E}_o$, $\bar{H}_o$ and the perturbed fields $\bar{E}$, $\bar{H}$ inside the waveguide satisfy the Maxwell equations, where the $e^{j\omega t}$ time dependency is assumed and ∇_t is the two-dimensional gradient operator in the transverse plane.

In the conventional way, by forming the expression [13]

$$\bar{H}_o^* \cdot \nabla_t \times \bar{E} + \bar{H} \cdot \nabla_t \times \bar{E}_o^* - \bar{E}_o^* \cdot \nabla_t \times \bar{H} - \bar{E} \cdot \nabla_t \times \bar{H}_o^*$$

and integrating this expression over the cross-section area S of the waveguide, the following relation for the change of the propagation